SIMULATION OF A SPATIAL SERVO-HYDRAULIC TEST FACILITY FOR SPACE STRUCTURES

K.-D. Leimbach, H. Hahn

Control Engineering and System Theory Group,
Department of Mechanical Engineering,
University of Kassel, Germany

ABSTRACT

In this paper different control concepts for servo-hydraulic test facilities are derived using exact linearization techniques. Based on different linear and nonlinear models of the test table and the actuator dynamics several nonlinear controllers of different complexity are derived. The closed loop system performance of the controlled servo-hydraulic test facility is tested in various computer simulations using both, standard test signals and large test signals as system inputs. The simulation results turn out, that in case of standard input signals the test facility controller must include a linear test table mechanics model and a nonlinear servohydraulic actuator model. Additional simulations demonstrate the robustness of the control concept selected for standard test signals with respect to variations of plant parameters.

INTRODUCTION (1)

Multi-axis servohydraulic test facilities are widely used for vibration testing of critical components of industrial equipment and of future spacecraft. First theoretical investigations of multi-axis test facility control concepts based on modern nonlinear control theory (exact linearization techniques) are (ref. 1) and (ref. 2). The control algorithms derived in (ref. 1, 2) are based on complex nonlinear component models of the test table mechanics and on linear component models of the hydraulic actuators. This paper extends the mathematical models of the servohydraulic actuators in (ref. 1, 2) from linear equations to highly nonlinear relations. Based on the different combinations of linear and nonlinear plant component models (Section 2) different control algorithms have been derived (Section 3). Using the different control algorithms of Section 3 various computer simulations have been made (Section 4) to find a trade-off between the controller complexity needed and the closed loop system behaviour desired. Additional computer simulations proof the robustness of the control concept selected with respect to plant parameter variations. The control algorithm selected provides an excellent system performance and turns out to be amazingly insensitive with respect to plant parameter variations.

NONLINEAR PLANT MODELING (2)

The test facility considered includes the following components (cf. 1):

- a rigid six degree of freedom test table with a rigid payload rigidly attached to it,
- l=6 or l=8 servohydraulic actuators and
- an integrated control system.

Test table and payload mechanics

The **nonlinear model equations** of the test table mechanics are (ref. 1)

$$\begin{aligned} \dot{x}_1 &= T(x_1)\cdot x_2 \\ M\left(J, r_{CP}^L, x_1\right)\cdot\dot{x}_2 &= J_{x1}^T(x_1)\cdot A_k\cdot p - J_{x1}^T(x_1)\cdot D_k\cdot J_{x1}(x_1)\cdot x_2 - n\left(J, r_{CP}^L, x_1, x_2\right) - q_G\left(r_{CP}^L, x_1\right) \end{aligned} \tag{1a}$$

where the first equation of (1a) includes the Poisson equations and the matrix $T(x_1)$ has been chosen as matrix of Bryant angles; M is the inertia matrix of the test facility, D_K and A_K are the diagonal matrices of the actuator damping coefficients and of the actuator piston areas, respectively; $x_1=\left[(r_P^R)^T, \eta^T\right]^T=\left[x_P^R, y_P^R, z_P^R, \varphi, \theta, \psi\right]^T \in \mathbb{R}^6$ is the position

and orientation vector of the spatial test facility, where the position vector $r_P^R=\left[x_P^R, y_P^R, z_P^R\right]^T$ is represented in inertial frame R and the orientations $\eta=[\varphi, \theta, \psi]^T$ are the Bryant angles; $x_2=\left[(\dot{r}_P^R)^T, (\omega_{LR}^L)\right]^T=\left[\dot{x}_P^R, \dot{y}_P^R, \dot{z}_P^R, p^L, q^L, r^L\right]^T \in \mathbb{R}^6$ is the velocity vector, where $\omega_{LR}^L=\left[p^L, q^L, r^L\right]^T$ is the angular velocity vector represented in body fixed frame L; $\dot{x}_2$ is the acceleration vector; n is the vector of the centrifugal forces and of the gyroscopic terms; q_G is the nonlinear vector of the gravitational force and the associated torque and $p:=[p_1, \cdots, p_l]^T \in \mathbb{R}^l$ is the vector of the actuator pressure differences. The nonlinear transformation matrix $J_{x1}^T(x_1)$ maps the actuator forces from joint fixed frames K_i into forces and torques represented in inertial frame R and in body fixed frame L, respectively (compare the representation of x_2). The associated **linear model equations** are

$$M\left(J, r_{CP}^L\right)\cdot\ddot{x}_1+T_d^T\cdot D_K\cdot T_d\cdot\dot{x}_1=T_d^T\cdot A_K\cdot p \tag{1b}$$

where T_d^T is the linearized transformation matrix J_{x1}^T, $J\in\mathbb{R}^{3,3}$ is the inertia tensor and $r_{CP}^L\in\mathbb{R}^3$ is the vector of the common center of gravity.

Servohydraulic actuators

The servohydraulic actuators are modeled by the **nonlinear equations** (ref. 3)

$$\dot{p}= B_2(p,x_V)\cdot x_u-C_H^{-1}\cdot Q_{BP}(p)-C_H^{-1}\cdot A_K\cdot J_{x_1}(x_1)\cdot x_2+B_1(p,x_V)\cdot x_V \quad \in\mathbb{R}^l \tag{2a}$$

where (for i=1,..., l, (l=6 in case of 6 actuators and l=8 in case 8 actuators acting onto the test table))

$$\begin{aligned} B_1(p,x_V) &:= C_H^{-1}\cdot K_\alpha\cdot\left\{Q_I(p,x_V)+Q_{II}(p,x_V)\right\} \in\mathbb{R}^{l,l} \\ B_2(p,x_V) &:= C_H^{-1}\cdot K_\alpha\cdot\left\{Q_{II}(p,x_V)-Q_I(p,x_V)\right\} \in\mathbb{R}^{l,l} \end{aligned} \tag{3}$$

and

$$\begin{aligned} K_\alpha &:= diag\left(\alpha_{Di}\cdot\pi\cdot d_i\cdot\sqrt{2/\rho}\right) \in\mathbb{R}^{l,l} \\ Q_I &:= diag\left(\sqrt{|p_0-p_i|/2}\cdot sign(p_0-p_i)\cdot\sigma(x_{vi}-x_{ui})\right) \in\mathbb{R}^{l,l} \\ Q_{II} &:= diag\left(\sqrt{|p_0+p_i|/2}\cdot sign(p_0+p_i)\cdot\sigma(-x_{vi}-x_{ui})\right) \in\mathbb{R}^{l,l} \\ Q_{BP} &:= \left(\alpha_{Di}\cdot A_{BPi}\sqrt{2/\rho\cdot|p_i|}\cdot sign(p_i)\right)_{i=1,\cdots,l}^T \in\mathbb{R}^l \\ C_H &:= \frac{L}{4\cdot B}\cdot A_K \quad (L \text{ actuator length, } B \text{ bulk modulus}). \end{aligned}$$

The associated **linear model equations** are

$$\dot{p}=C_H^{-1}\cdot\left[Q_x\cdot x_V+Q_P\cdot p-A_k\cdot J_{x1}(x_1)\cdot x_2\right] \in\mathbb{R}^l \tag{2b}$$

where x_V is the vector of servovalve piston positions $x_V=[x_{v1}, \cdots, x_{vl}]^T \in\mathbb{R}^l$ and $C_H, Q_P, Q_x\in\mathbb{R}^{l,l}$ are the diagonal matrices of the actuator hydraulic capacities, servovalve pressure coefficients and servovalve displacement coefficients, respectively. The plant simulation includes the following model equations of the servovalve mechanics

$$\ddot{x}_{vi}+2\cdot\zeta_{vi}\cdot\omega_{vi}\cdot\dot{x}_{vi}+\omega_{vi}^2\cdot x_{vi}=k_{vi}\cdot\omega_{vi}^2\cdot u_i \in\mathbb{R}^1, \text{ (i=1, ..., } l) \tag{4a}$$

with $\zeta_{vi}=0.7$ and $f_V=\omega_V/2\pi$. In (4a) $u=[u_1, \cdots, u_l]^T\in\mathbb{R}^l$ is the system input. The control laws will be derived taking into account the following simplified servovalve model

$$x_{vi}=k_{vi}\cdot u_i \in\mathbb{R}^1, \text{ (i=1,..., } l). \tag{4b}$$

NONLINEAR CONTROLLER DESIGN (3)

The subsequent nonlinear controller design is based on the trivial servovalve dynamics of (4b), where the servovalve dynamics included in (4a) has been neglected (ref. 1). This tremendously simplifies the controller design. This simplification will be justified by the subsequent simulation results. Then the choice of the system output $y=h(x_1):=x_1$ leads to a well defined vector relative degree of $[3,3,3,3,3,3]$ (in case of l=6 servo-hydraulic actuators). Using in addition the system output $y=x_1$ yields the normal form representation (5) of the simplified plant which provides the basis for the subsequent controller designs.

$$\begin{aligned} \dot{z}_1 &:= \dot{y} = \dot{x}_1 = z_2 \\ \dot{z}_2 &:= \ddot{y} = \ddot{x}_1 = z_3 \\ \dot{z}_3 &:= \alpha_j + \beta_j \cdot u \,. \end{aligned} \tag{5}$$

where $\dot{z}_1 = z_2$, $\dot{z}_2 = z_3$ and $\dot{z}_3$ are the spatial test table velocity, acceleration and jerk, respectively, and α_j, β_j (j= I, II, III, IV) are the different normal form plant relations (7a), (7b), (7c), (7d) associated to the plant models collected in Table 1, respectively.

Based on the system equations (5) the nonlinear controller design is straight forward (ref. 1):

$$u = \beta_j^{-1} \cdot (v - \alpha_j) \tag{6a}$$

where for l=6 β_j^{-1} is the inverse of β_j, and for l=8 β_j^{-1} is defined as the right inverse of β_j.

A suitable choice of K_0, K_1, $K_2 \in \mathbb{R}^{6,6}$ in

$$v := \dot{z}_{3d} - K_2 \cdot (z_3 - z_{3d}) - K_1 \cdot (z_2 - z_{2d}) - K_0 \cdot (z_1 - z_{1d}) \tag{6b}$$

guarantees a stable error dynamics of the closed loop system, where $\dot{z}_{3d}$, z_{3d}, z_{2d}, z_{1d} are the desired jerk, acceleration, velocity and position set point signals, respectively. The measurements required in (6) are the test table degree of freedom positions/orientations z_1, velocities z_2 and accelerations z_3. The plant nonlinearities are compensated by α_j and β_j^{-1} (compare (6a)) where, the different representations of the controller relations α_j and β_j^{-1} depend on the plant component model equations of Table 1. The different controllers investigated are (comp. Table 1):

Case j=I (using (1b) and (2b)):

$$\begin{aligned} \alpha_I &= M^{-1} \cdot T_d^T \cdot A_K \cdot \left\{ C_H^{-1} \cdot Q_P \cdot p - C_H^{-1} \cdot A_K \cdot T_d \cdot \dot{x}_1 \right\} - M^{-1} \cdot T_d^T \cdot D_K \cdot T_d \cdot \ddot{x}_1 \\ \beta_I &= M^{-1} \cdot T_d^T \cdot A_K \cdot C_H^{-1} \cdot Q_P \cdot K_V, \end{aligned} \tag{7a}$$

Case j=II (using (1b) and (2a)):

$$\begin{aligned} \alpha_{II} &= M^{-1} \cdot T_d^T \cdot A_K \cdot \left\{ B_2 \cdot x_u - C_H^{-1} \cdot Q_{BP} - C_H^{-1} \cdot A_K \cdot T_d \cdot \dot{x}_1 \right\} - M^{-1} \cdot T_d^T \cdot D_K \cdot T_d \cdot \ddot{x}_1 \\ \beta_{II} &= M^{-1} \cdot T_d^T \cdot A_K \cdot C_H^{-1} \cdot K_\alpha \cdot \{ Q_I + Q_{II} \} \cdot K_V, \end{aligned} \tag{7b}$$

Case j=III (using (1a) and (2b)):

$$\begin{aligned} \alpha_{III} &= \frac{d^3 x_1(p, x_1, x_2)}{dt^3} = \left[\frac{\partial \ddot{x}_1}{\partial p} \cdot \dot{p} + \frac{\partial \ddot{x}_1}{\partial x_1} \cdot \dot{x}_1 + \frac{\partial \ddot{x}_1}{\partial x_2} \cdot \dot{x}_2 \right] \\ \beta_{III} &= T \cdot M^{-1} \cdot T_d^T \cdot A_K \cdot C_H^{-1} \cdot Q_P \cdot K_V, \end{aligned} \tag{7c}$$

Case j=IV (using (1a) and (2a)):

$$\begin{aligned} \alpha_{IV} &= \frac{d^3 x_1(p, x_1, x_2)}{dt^3} = \left[\frac{\partial \ddot{x}_1}{\partial p} \cdot \dot{p} + \frac{\partial \ddot{x}_1}{\partial x_1} \cdot \dot{x}_1 + \frac{\partial \ddot{x}_1}{\partial x_2} \cdot \dot{x}_2 \right] \\ \beta_{IV} &= T \cdot M^{-1} \cdot T_d^T \cdot A_K \cdot C_H^{-1} \cdot K_\alpha \{ Q_I + Q_{II} \} \cdot K_V \end{aligned} \tag{7d}$$

where

$$\ddot{x}_1 = \frac{\partial}{\partial x_1}\left(T(x_1)\cdot x_2\right)\cdot \dot{x}_1 + T(x_1)\cdot\left\{M^{-1}(x_1)\cdot\left[J_{x1}^T(x_1)\cdot A_K\cdot p - J_{x1}^T(x_1)\cdot D_K\cdot J_{x1}(x_1)\cdot x_2 - n(x_1, x_2) - q_G(x_1)\right]\right\}. \tag{8}$$

Both, the controller complexity and the closed loop system behaviour severely depend on the plant models included in the control law design. Control laws based on **nonlinear test table equations** of motion (1a) (Case III and Case IV) are extreme complex and lengthy (more than one hundred DIN A4 pages of length, ref. 1). This is due to the partial derivatives of $\ddot{x}_1$ with respect to p, x_1 and x_2 in (7c) and (7d), where $\ddot{x}_1$ is defined in (8). Control laws based on **linear test table mechanics** (1b) are much less complex (less than 5 pages of length (Cases I and II)). The simulation results of Section 4 show which component models must be included in the control law design in order to achieve a satisfactory control loop behaviour using different test signal levels.

SIMULATION RESULTS (4)

Variation of control concepts (test facility with *l*=6 servo-hydraulic actuators)

The subsequent simulations tend to find a trade-off between the closed loop system behaviour and the complexity of the controller to be implemented. Apart from Simulation No. 5b and 5c (comp. Table 2) all simulations are based on the ideal servovalve model (4a) with an upper limit frequency of f_v=1000 *Hz*. As discussed in Section 3 the controller complexity severely depends on the plant model equations taken into account in the controller design. The nonlinear plant (1a), (2a) and (4a) together with the different control laws of Table 1 have been investigated in computer simulations using both, standard transient test signals for vibration testing of space structures used in industry (as shown in Figures 2a and 4a) and large test signals (as shown in Figures 3a and 5a) derived from the standard test signals in order to simulate large spatial motions. A control law based on **linear plant models** of both, the test table mechanics and the actuator dynamics (comp. Table 1, Case I and Equation (7a)) provides in case of standard test signals (cf. 2a) large couplings among the test facility degrees of freedom and a poor tracking behaviour in the y- and z-degrees of freedom (cf. 2b and Simulation No. 1a of Table 2). A control law based on **linear actuator dynamics** and on **nonlinear test table mechanics** (comp. Table 1, Case III and Equation (7c)) provides in case of standard test signals the same poor tracking behaviour in the y- and z-degrees of freedom and large couplings among the test facility degrees of freedom (cf. 2c and Simulation No. 1b of Table 2). Even less quality results hold for simulations using large test signals (cf. 3a) in case of a control concept based on **linear plant models** (cf. 3b and Simulation No. 2a of Table 2) and in case of a control concept based on **linear actuator dynamics** and on **nonlinear test table mechanics** (cf. 3c and Simulation No. 2b of Table 2). The unwanted couplings among all test table degrees of freedom may destroy the payloads to be tested. Both, the tracking and the decoupling behaviour of the test facility have been improved by taking into account **linear test table mechanics** and **nonlinear actuator dynamics** in the control law design (comp. Table 1, Case II and Equation (7b)) using standard test signals (cf. 4b and Simulation No. 3a of Table 2). A control concept based on **nonlinear test table mechanics** and on **nonlinear actuator dynamics** (comp. Table 1, Case IV and Equation (7d)) provides the same excellent tracking and decoupling behaviour using standard test signals (cf. 4c and Simulation No. 3b of Table 2). In case of large test signals the control concept based on **linear test table mechanics** and on **nonlinear actuator dynamics** provides both, a poor tracking behaviour in the y- and z-degrees of freedom and large couplings among all degrees of freedom (cf. 5b and Simulation No. 4a of Table 2). A control concept based on **nonlinear test table mechanics** and on **nonlinear actuator dynamics** provides an ideal tracking and decoupling behaviour even in case of large test signals (cf. 5c and Simulation No. 4b of table 2). From the previous computer simulations the following conclusions have been drawn:

- Using **standard test signals** (cf. 2a) a controller design based on **linear test table mechanics** and on **nonlinear hydraulic actuator models** provides a satisfactory transient and decoupling behaviour of the controlled test facility.

- In case of **large test signals** (cf. 3a) both, the **nonlinear test table mechanics** and the **nonlinear actuator dynamics** must be included in the controller design. This, however, generates controllers of extreme high complexity (comp. Table 1, Case IV).

Additional computer simulation results with **unstructured uncertainties** are shown in Figure 6. The plant simulation still includes the nonlinear test table mechanics (1a), the nonlinear servo-hydraulic actuator dynamics (2a) and the servovalve mechanics model (4a). The control concept selected is based on linear test table mechanics (1b), on nonlinear actuator dynamics (2a) and on the simplified servovalve model (4b) which doesn't take into account any servovalve dynamics. In the simulations the **upper servovalve limit frequency** f_v of the plant model is varied from f_v=100 *Hz* to f_v=1000 *Hz*. In case of an unrealistic upper limit frequency of f_v=1000 *Hz* the transmission behaviour of

the test facility is nearly ideal (cf. 6a). As a consequence the valve dynamics (4a) can be omitted from the controller design in this case. For f_v=300 *Hz* the transmission behaviour is of reduced quality but still acceptable (cf. 6b). For f_v=100 *Hz* the transmission behaviour is further reduced in comparison to Figure 6b and no longer acceptable (cf. 6c). On the other hand, Figure 6b shows, that an exact linearization controller design for a test facility including high response valves with an upper limit frequency f_v of about 300 Hz may be drastically simplified by omitting the servovalve dynamics in the control law design. The resulting control errors are of minor practical importance.

Robustness with respect to plant parameter variations (test facility with *l*=8 servo-hydraulic actuators)

In industrial practice usually not all plant parameters to be implemented in the control algorithms are known exactly. As a consequence, the plant parameter values used in the control law may deviate from the actual parameter values of the plant. The influence of those parametric discrepancies between associated plant and controller parameters is investigated subsequently by the second set of computer simulations (comp. Table 3). The **control concept** selected for these investigations is based on **linear test table mechanics** (1b), on **nonlinear servohydraulic actuator dynamics** (2a) and on the servovalve model (4b). Standard transient test signals used in industry for vibration testing of space structures are used throughout these investigations and the valve limit frequency of the plant is set to f_v=1000 *Hz*. Each of the following variations of a controller parameter is counted with respect to the associated nominal value of this controller parameter which is identical to the associated plant parameter. Variations of the **servovalve amplification factor** k_{vi} by 10 % in Figure 7b produce only slight modifications in the tracking behaviour of the system. Only variations of k_{vi} of about 50 % or more have significant influence on the tracking behaviour (cf. 7c). The decoupling of the test table degrees of freedom is insensitive even with respect to large variations of k_{vi}. A variation of k_{vi} simultaneously stands for a variation of various other **controller amplifications factors**. Variations of the **bulk modulus B** which stand for variations of the compressibility due to temperature variations and due to oil contaminations caused by air bubbles are shown in Figure 8. The tracking behaviour is only influenced slightly by variations of B of 50% (cf. 8b). Unrealistic variations of B by a factor four or more modify the tracking behaviour significantly according to Figure 8c. In Figure 9b the common **mass *m* of the test table and payload** is modified by a factor 1/2. This drastic mass variation again does not severely influence both, the tracking and the coupling behaviour of the system. Only unrealistic variations of *m* by a factor four or more have significant influence on the system behaviour (cf. 9c). Variations of all **moments and products of inertia** by a factor 1/2 or 4 have no significant effect on the system behaviour (cf. 10b and cf. 10c). Variations of the **common center of gravity** r_{CP}^L of the test facility and payload are shown in Figure 11. Simultaneous huge modifications of all components of the vector r_{CP}^L from reference point P to center of gravity C (for fixed P) by a factor of 1/2 are shown in Figure 11b. They don't affect the tracking behaviour and only provide slight couplings among the test table degrees of freedom. Only unrealistic variations of r_{CP}^L by a factor four or more show significant modifications of the transmission behaviour of the system (cf. 11c). The nominal plant model equations (5) did not include nonlinear **friction forces** due to dry friction in the hydraulic actuators and in the joints attached to those. As a consequence those friction forces have not been taken into account in the nonlinear control law design. Figure 12 shows simulation results including nonlinear friction forces of different absolute values in the plant model. Friction forces F_R smaller than 1 kN don't provide relevant influences upon the system behaviour (cf. 12b). Friction forces of the order of F_R=3 kN don't affect the tracking behaviour. They introduce coupling effects of some test facility degrees of freedom (cf. 12c). Extreme high friction forces in the servo-hydraulic actuators are avoided in practice by using actuators with hydrostatic bearings. The above numerical sensitivity analysis of the control system demonstrates that the exact linearization approach is much less sensitive to plant parameter variations and to controller parameter variations than often predicted.

CONCLUSION (5)

This paper presents different control designs for spatial multi-axis test facilities with six or eight servo-hydraulic actuators. The various control designs investigated are based on exact linearization techniques taking into account different combinations of linear and nonlinear plant component models. The system performance of the multi-axis test facility controlled by different control concepts has been tested in various computer simulations. In case of standard transient input signals a nonlinear controller design based on nonlinear servo-hydraulic actuator models and on linear test table mechanics is sufficient to achieve an excellent tracking and decoupling behaviour. The amount of the associated controller implementation is kept within acceptable limits. In case of large spatial transient motions of the test table with high velocities and accelerations, the control concept must take into account both, the nonlinear actuator dynamics and the nonlinear test table mechanics. This yields control algorithms of several hundred pages of length which require an enormous amount of hardware implementation work. Additional simulation results demonstrate considerable robustness of the closed loop system with respect to plant parameter variations and with respect to unmodeled servovalve dynamics in the controller.

REFERENCES (6)

1. Hahn, H., Leimbach, K.-D.:. Nonlinear Control and Sensitivity Analysis of a Spatial Multi-Axis Servohydraulic Test Facility. Proceedings of the 32nd IEEE CDC, San Antonio 1993.

2. Hahn, H., Leimbach, K.-D. and Zhang, X.: Nonlinear Control of a Spatial Multi-Axis Servo-Hydraulic Test Facility. IFAC World Congress, Sydney 1993.

3. Hahn, H.: Theoretische Modellbildung Elektro-Servohydraulischer Antriebe, Lecture Notes, IMAT-Report 2, University of Kassel (ISSN 0939-8678), 1991.

Table 1. Plant models included in the controller design.

Test Signal Level	models of mechanical components included in the control law design	
	linear (1b)	nonlinear (1a)
models of hydraulic components included in the control law design: linear (2b)	**Case I** (α_I, β_I) *(low controller complexity)*	**Case III** (α_{III}, β_{III}) *(high controller complexity)*
models of hydraulic components included in the control law design: nonlinear (2a)	**Case II** (α_{II}, β_{II}) *(low controller complexity)*	**Case IV** (α_{IV}, β_{IV}) *(extreme high controller complexity)*

Table 2. Computer simulation runs of the controlled servo-hydraulic test facility (with 6 servo-hydraulic actuators) using different control algorithms. The control algorithms are based on different plant component models and nominal test facility model data.

Simulation No.	Test signal	Control concepts				Grading of the closed loop system performance	
		Case I lin mech / lin hyd	Case II lin mech / nl hyd	Case III nl mech / lin hyd	Case IV nl mech / nl hyd	tracking	decoupling
1a)	standard (Figure 2a)	Figure 2b				-	- -
1b)				Figure 2c		-	- -
2a)	large (Figure 3a)	Figure 3b				- -	- -
2b)				Figure 3c		- -	- -
3a)	standard (Figure 4a)		Figure 4b			+ +	+ +
3b)					Figure 4c	+ +	+ +
4a)	large (Figure 5a)		Figure 5b			-	- -
4b)					Figure 5c	+ +	+ +
5a)	standard (Figure 4a)		Figure 6a f_y=1000 Hz			+ +	+ +
5b)			Figure 6b f_y=300 Hz			+ +	+ +
5c)			Figure 6c f_y=100 Hz			+	-

lin mech (nl mech) : linear (nonlinear) model of the test table mechanics
lin hyd (nl hyd) : linear (nonlinear) model of the servo-hydraulic actuators

++: excellent tracking / decoupling behaviour
+: good tracking / decoupling behaviour
-: poor tracking / decoupling behaviour
- -: very poor tracking / decoupling behaviour

Table 3. Computer simulation runs of the controlled servo-hydraulic test facility (with 8 servo-hydraulic actuators) for plant parameter variations using the control law (7b) and standard test signals.

Simulation No.	Test signal	Control concept	Variation	Variation factor	Figure	Grading of the closed loop system performance	
						tracking	decoupling
6a)	↑ standard (Figure 2a) ↓	↑ Case II lin mech / nl hyd ↓	servo valve gain factor k_v	1 (nominal value)	7a	++	++
6b)				0.9	7b	+	++
6c)				1.5	7c	+	+
7a)			bulk modulus B	1 (nominal value)	8a	++	++
7b)				0.5	8b	+	+
7c)				4	8c	-	+
8a)			common mass of test table and pay-load m	1 (nominal value)	9a	++	++
8b)				0.5	9b	+	+
8c)				4	9c	--	--
9a)			inertia tensor J	1 (nominal value)	10a	++	++
9b)				0.5	10b	++	++
9c)				4	10c	++	++
10a)			center of gravity of test table and pay-load r_{CP}^L	1 (nominal value)	11a	++	++
10b)				0.5	11b	++	+
10c)				4	11c	-	--
11a)			dry friction force within the actuators F_R	F_R=0 kN	12a	++	++
11b)				F_R=1 kN	12b	++	+
11c)				F_R=3 kN	12c	++	-

lin mech : linear model of the test table mechanics
nl hyd : nonlinear model of the servo-hydraulic actuators

++ : excellent tracking / decoupling behaviour
+ : good tracking / decoupling behaviour
- : poor tracking / decoupling behaviour
-- : very poor tracking / decoupling behaviour

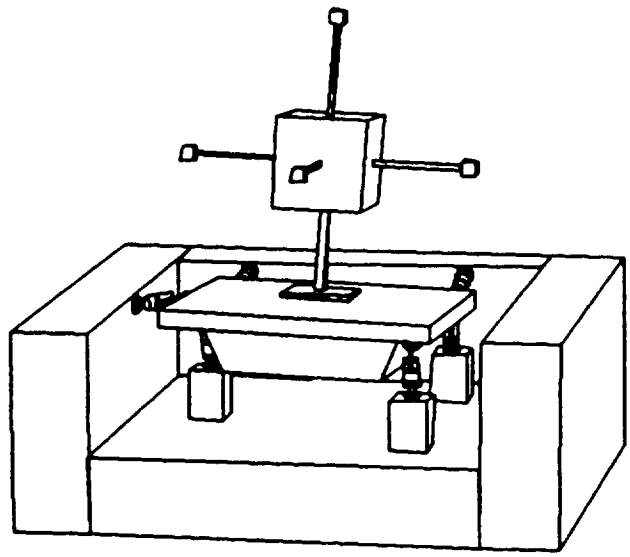

Figure 1: Computer drawing of a multi-axis servo-hydraulic test facility.

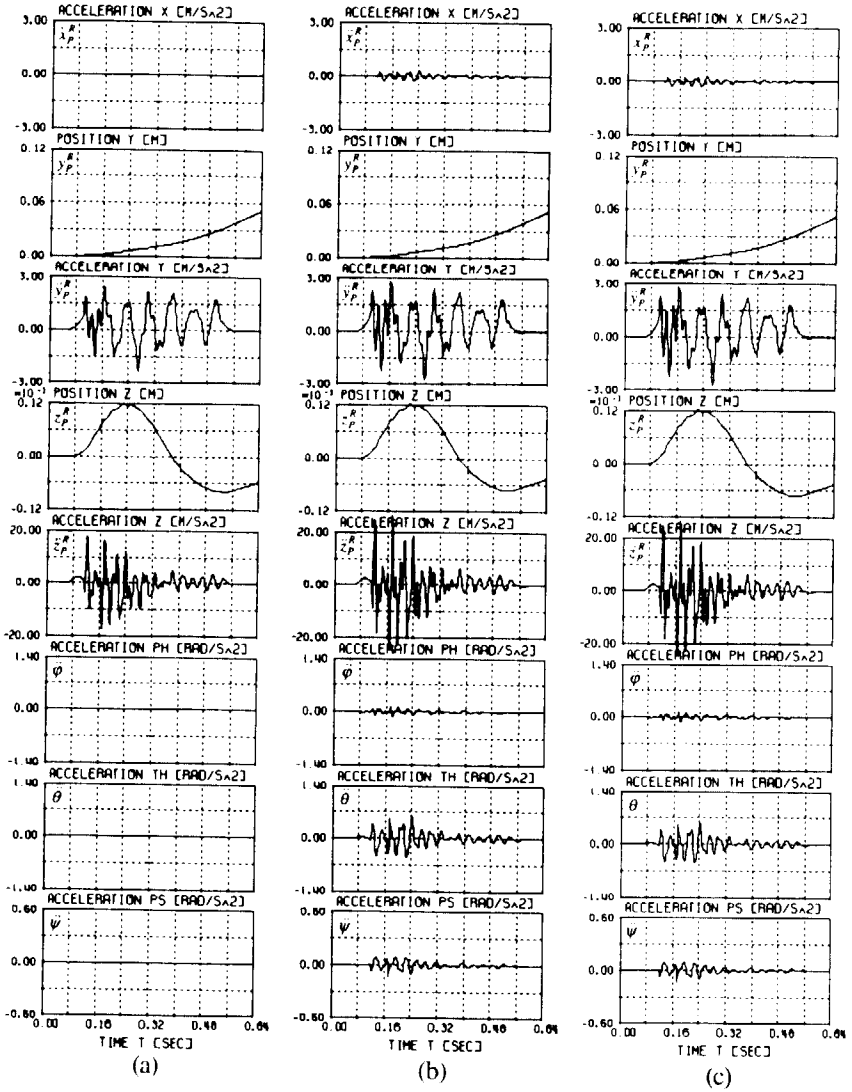

(a) (b) (c)

Figure 2: Computer simulation results of the test facility degrees of freedom using different control concepts of Table 1:

(a) standard set point signals used in industry,
(b) control concept based on Case I (comp. Table 1 and Table 2),
(c) control concept based on Case III (comp. Table 1 and Table 2).

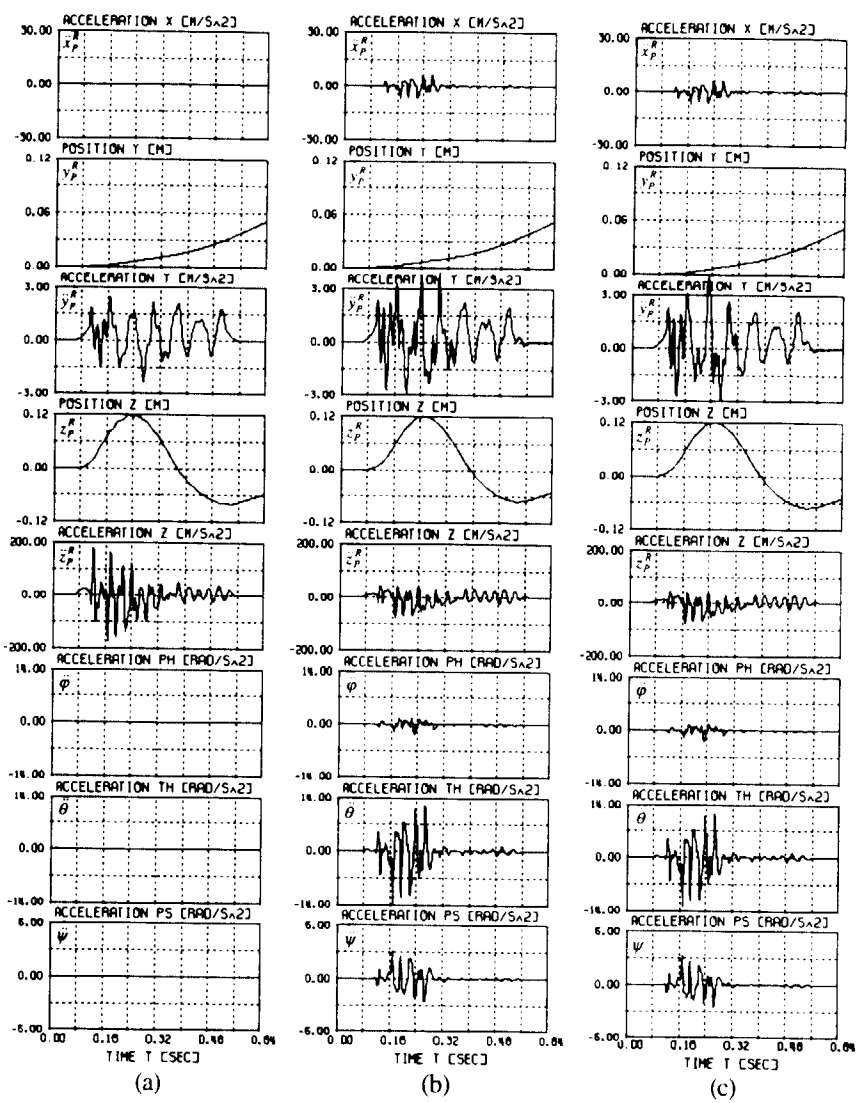

(a) (b) (c)

Figure 3: Computer simulation results of the test facility degrees of freedom using different control concepts of Table 1:

(a) large set point signals,
(b) control concept based on Case I (comp. Table 1 and Table 2),
(c) control concept based on Case III (comp. Table 1 and Table 2).

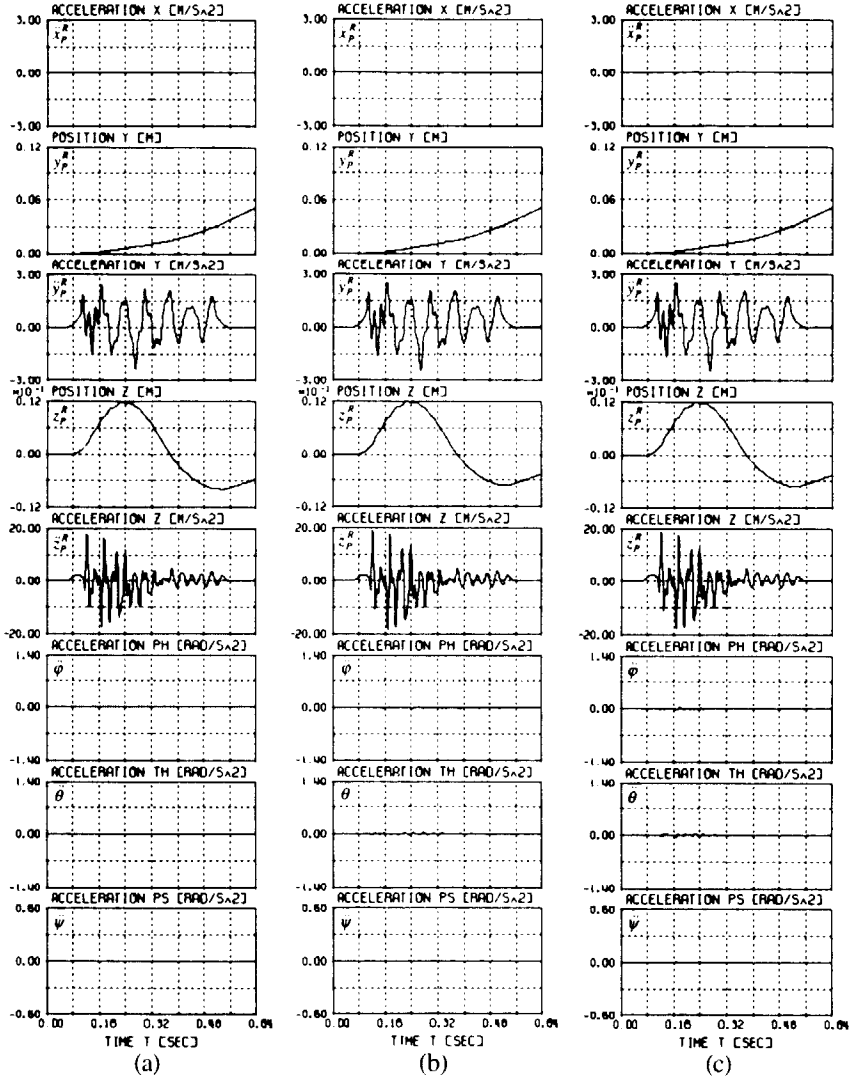

(a) (b) (c)

Figure 4: Computer simulation results of the test facility degrees of freedom using different control concepts of Table 1:

(a) standard set point signals used in industry,
(b) control concept based on Case II (comp. Table 1 and Table 2),
(c) control concept based on Case IV (comp. Table 1 and Table 2).

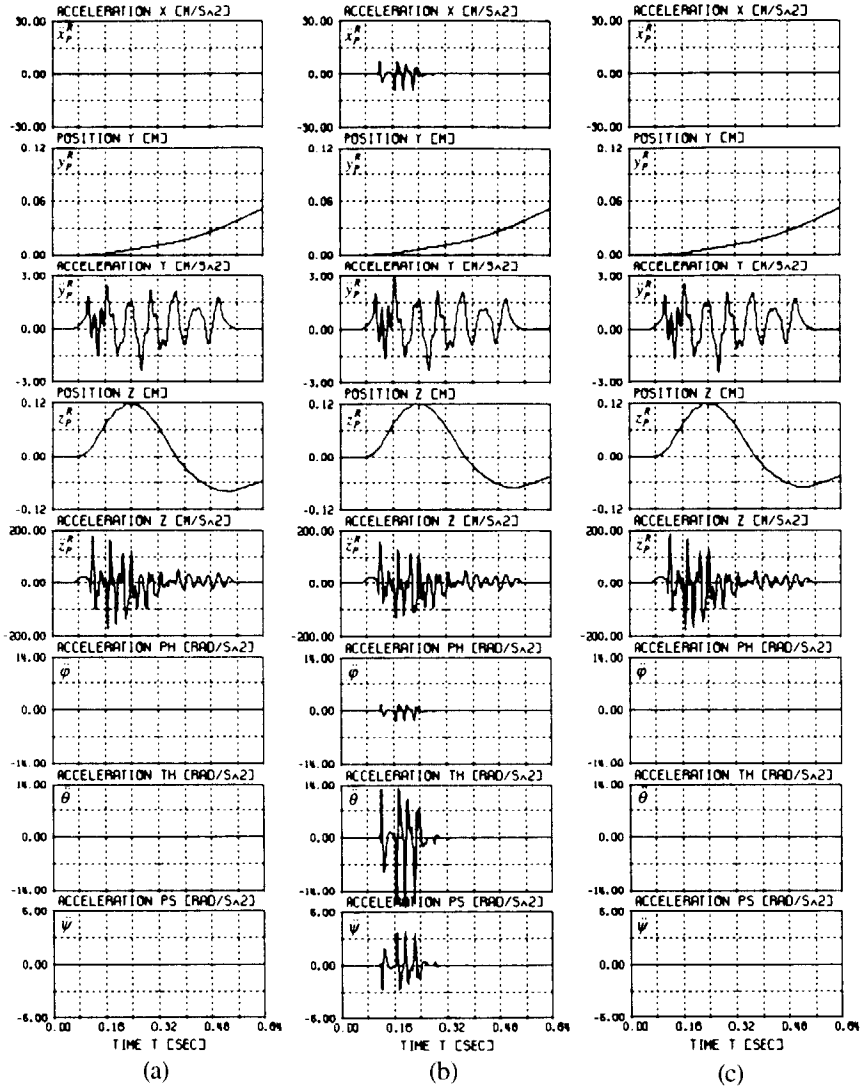

(a) (b) (c)

Figure 5: Computer simulation results of the test facility degrees of freedom using different control concepts of Table 1:

(a) large set point signals,
(b) control concept based on Case II (comp. Table 1 and Table 2),
(c) control concept based on Case IV (comp. Table 1 and Table 2).

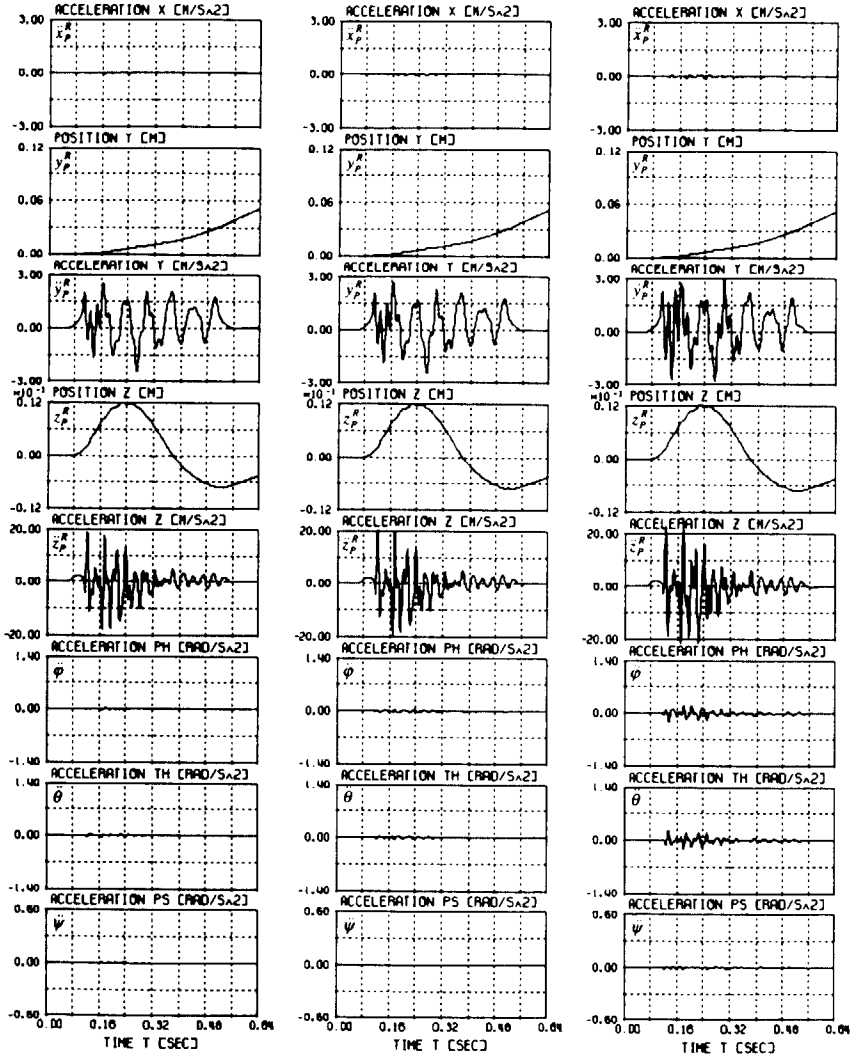

(a) (b) (c)

Figure 6: Computer simulation results of the test facility degrees of freedom taking into account unmodeled valve dynamics f_v:

(a) f_v =1000 Hz (control concept of Case II, Table 1),
(b) f_v =300 Hz (control concept of Case II, Table 1),
(c) f_v =100 Hz (control concept of Case II, Table 1).

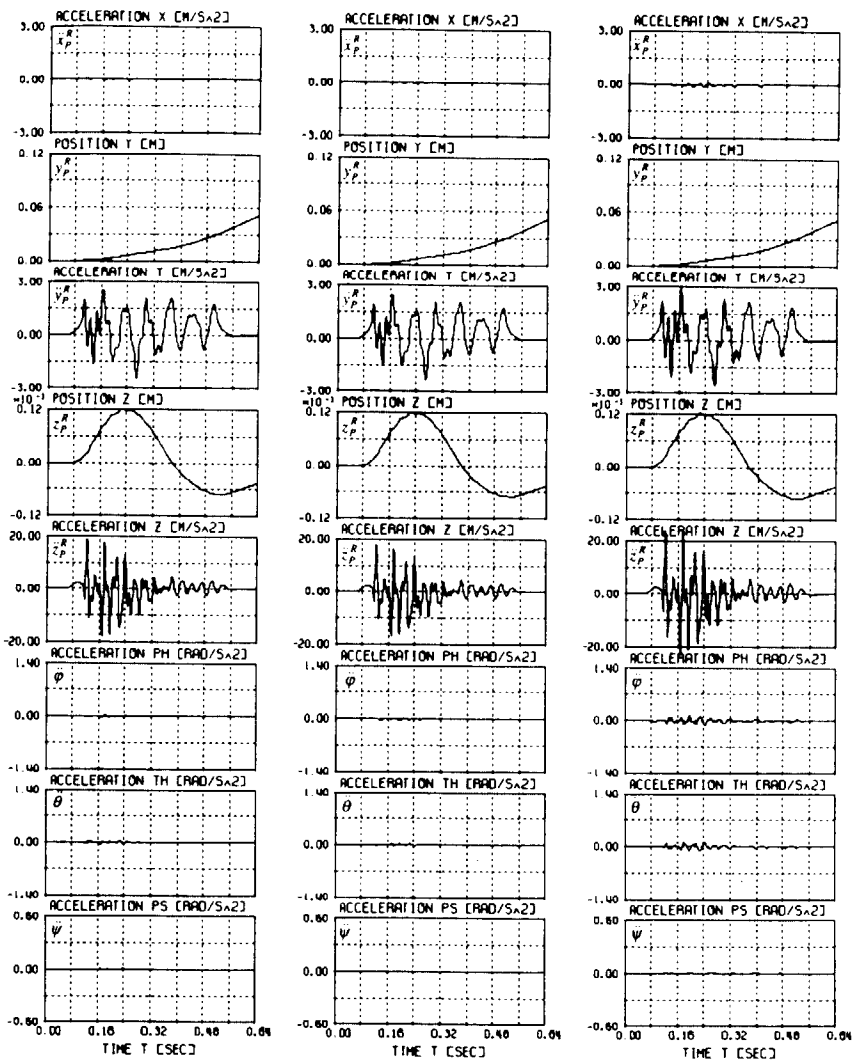

(a) (b) (c)

Figure 7: Computer simulation results of the test facility degrees of freedom taking into account plant parameter variations of the servovalve gains k_{vi} (control concept of Case II, Table 1):

(a) nominal values of k_{vi} (comp.Table 3),
(b) variation of k_{vi} by a factor of 0.9 (comp.Table 3),
(c) variation of k_{vi} by a factor of 1.5 (comp. Table 3).

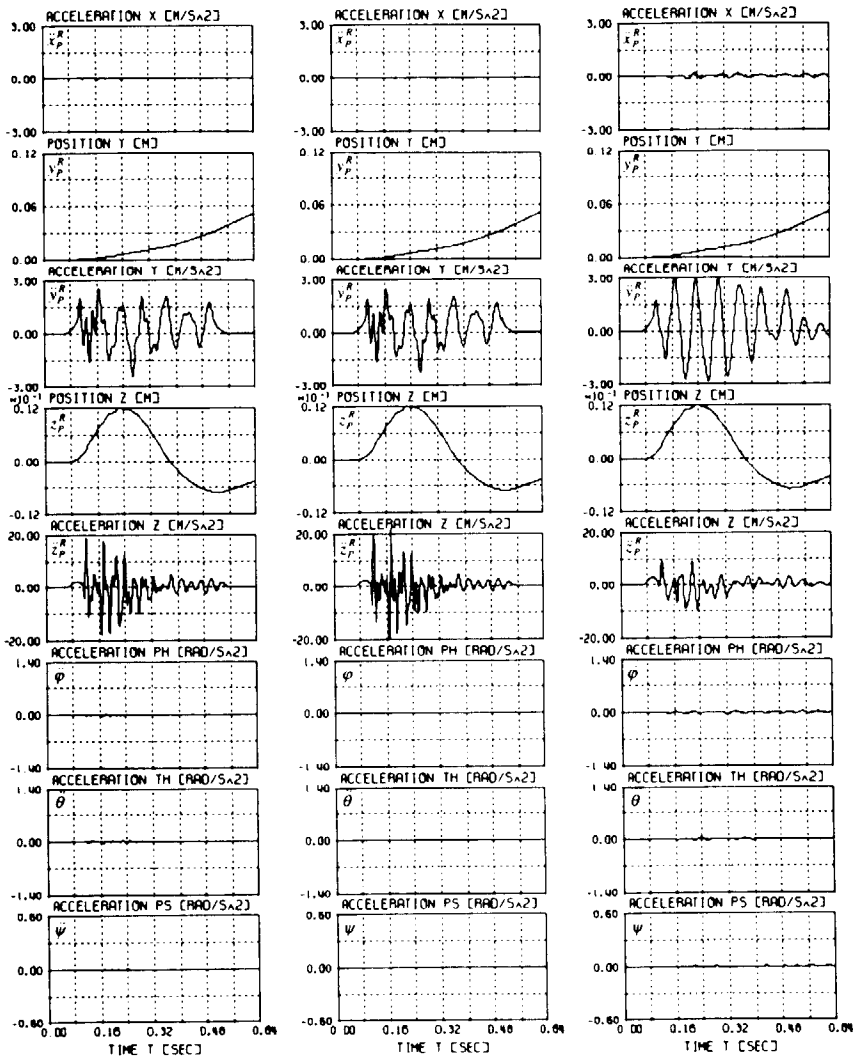

(a) (b) (c)

Figure 8: Computer simulation results of the test facility degrees of freedom taking into account plant parameter variations of the bulk modulus B (control concept of Case II, Table 1):

(a) nominal value of B (comp. Table 3),
(b) variation of B by a factor of 0.5 (comp.Table 3),
(c) variation of B by a factor of 4 (comp. Table 3).

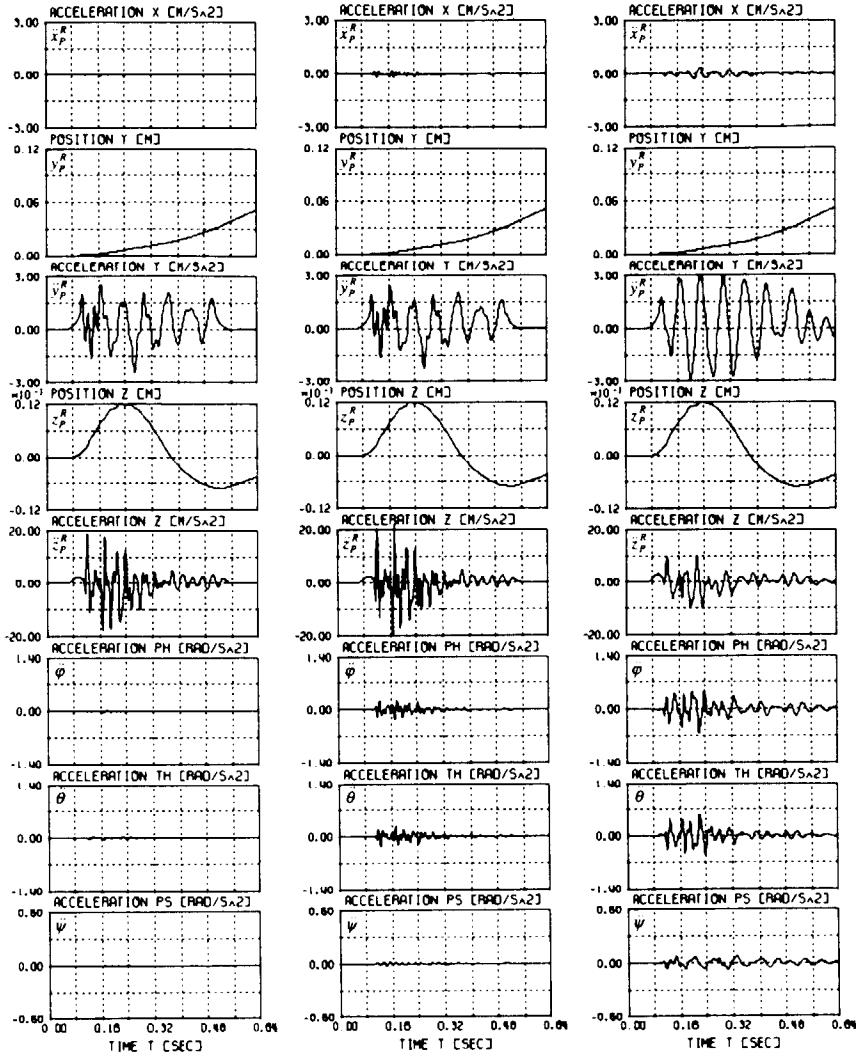

(a) (b) (c)

Figure 9: Computer simulation results of the test facility degrees of freedom taking into account plant parameter variations of the common mass m of the test table and payload (control concept of Case II, Table 1):

(a) nominal value of m (comp. Table 3),
(b) variation of m by a factor of 0.5 (comp.Table 3),
(c) variation of m by a factor of 4 (comp. Table 3).

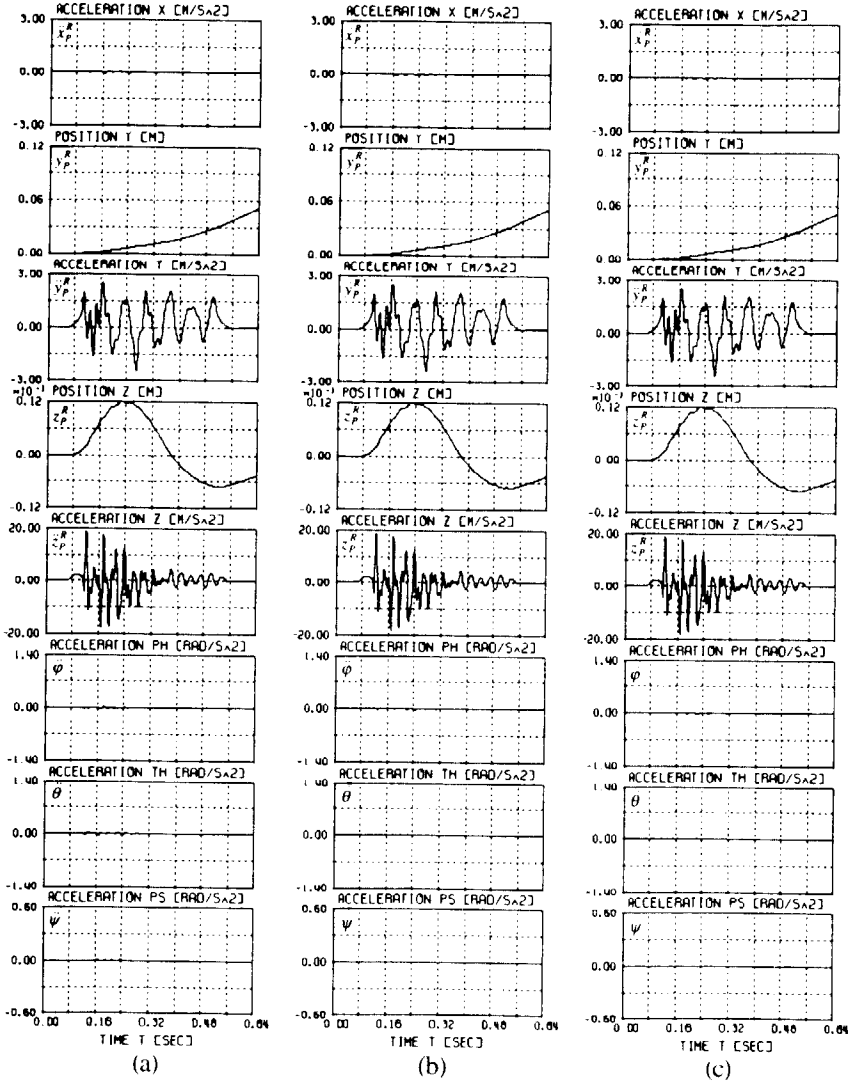

Figure 10: Computer simulation results of the test facility degrees of freedom taking into account plant parameter variations of the elements of the inertia tensor J (control concept of Case II, Table 1):

(a) nominal values in J (comp. Table 3),
(b) variation of the elements in J by a factor of 0.5 (comp. Table 3),
(c) variation of the elements in J by a factor of 4 (comp. Table 3).

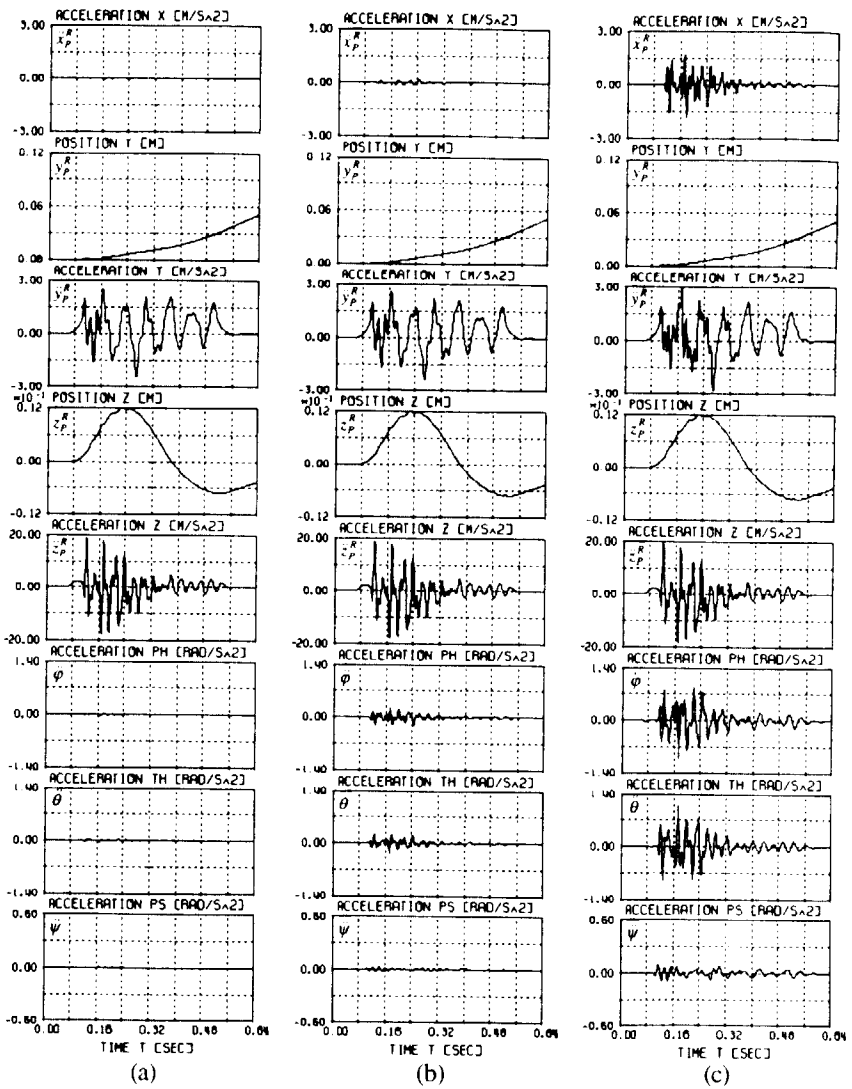

Figure 11: Computer simulation results of the test facility degrees of freedom taking into account plant parameter variations of the common center of gravity r_{CP}^{L} (control concept of Case II, Table 1):

(a) nominal value of r_{CP}^{L} (comp. Table 3),
(b) variation of r_{CP}^{L} by a factor of 0.5 (comp. Table 3),
(c) variation of r_{CP}^{L} by a factor of 4 (comp. Table 3).

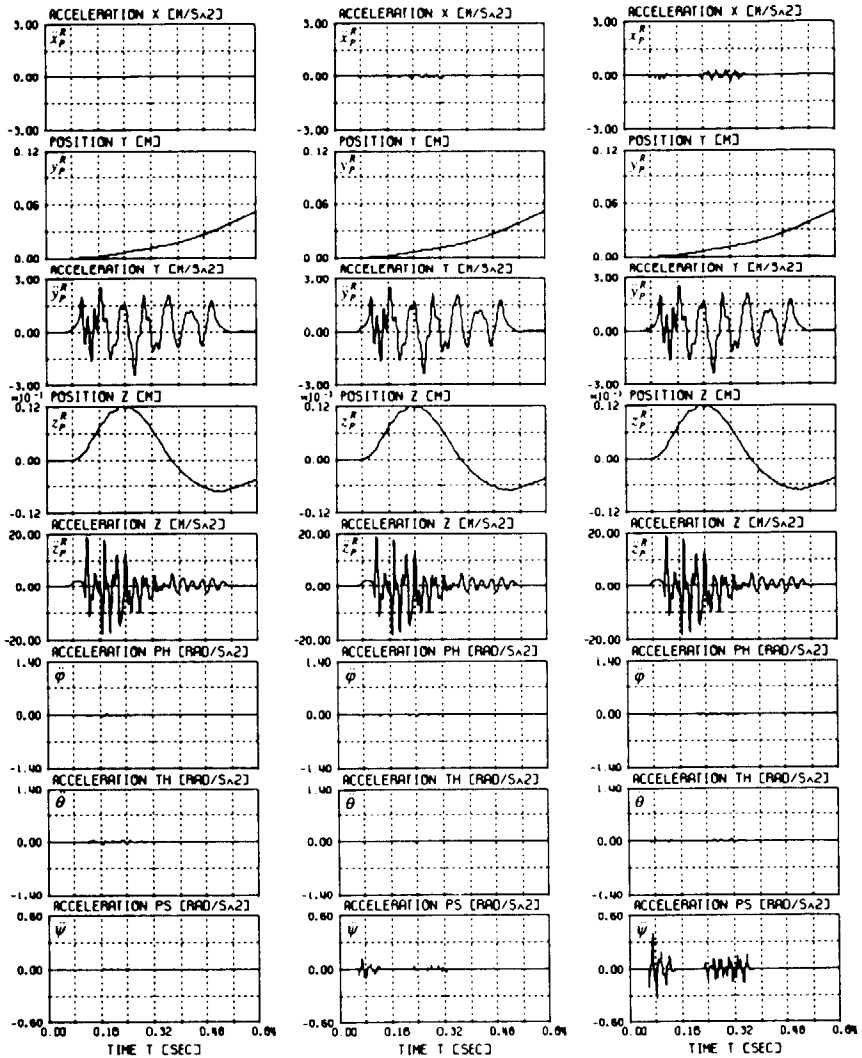

Figure 12: Computer simulation results of the test facility degrees of freedom taking into account dry friction forces F_R within the actuators and the joints attached to those (control concept of Case II, Table 1):

(a) dry friction force F_R= 0 kN (comp. Table 3),
(b) dry friction force F_R= 1 kN (comp. Table 3),
(c) dry friction force F_R= 3 kN (comp. Table 3).